TOXICOLOGICAL SCIENCES **113(1)**, 198–206 (2010)
doi:10.1093/toxsci/kfp226
Advance Access publication October 4, 2009

2,3,7,8-Tetrachlorodibenzo-*p*-dioxin Inhibits Fibroblast Growth Factor 10-Induced Prostatic Bud Formation in Mouse Urogenital Sinus

Chad M. Vezina,*,†,[1] Heather A. Hardin,‡ Robert W. Moore,†,‡ Sarah H. Allgeier,†,‡ and Richard E. Peterson†,‡

**Department of Comparative Biosciences, School of Veterinary Medicine; †Molecular and Environmental Toxicology Center; and ‡School of Pharmacy, University of Wisconsin, Madison, Wisconsin 53705-2222*

[1] To whom correspondence should be addressed at Department of Comparative Biosciences, Animal Health and Biomedical Sciences Building, 1656 Linden Drive, Madison, WI 53706. Fax: (608) 262-7420. E-mail: cmvezina@wisc.edu.

Received August 7, 2009; accepted September 9, 2009

2,3,7,8-Tetrachlorodibenzo-*p*-dioxin (TCDD) dorsalizes the pattern of prostatic buds developing from the urogenital sinus (UGS) of male fetal mice, causing some buds to form in inappropriate positions while blocking formation of others. This teratogenic TCDD action significantly reduces prostate main duct number and causes ventral prostate agenesis in exposed males. The purpose of this study was to determine whether inhibition of fibroblast growth factor 10 (FGF10) signaling is mechanistically linked to mouse prostatic budding impairment by TCDD. *In utero* TCDD exposure induced aryl hydrocarbon receptor–responsive cytochrome P450 1b1 messenger RNA (mRNA) in ventral UGS regions where *Fgf10* and fibroblast growth factor receptor 2 (*Fgfr2*) mRNA were expressed and where budding was most severely inhibited by TCDD. However, TCDD exposure did not reduce *Fgf10* or *Fgfr2* mRNA abundance in the UGS or alter their distribution. Addition of FGF10 protein to UGS organ culture media increased the abundance of UGS basal epithelial cells immunopositive for phosphorylated extracellular signal–regulated kinase (ERK). FGF10 also increased the number of 5-bromo-2′-deoxyuridine (BrdU)-labeled UGS epithelial cells and increased the number of prostatic buds formed per UGS. Addition of TCDD to UGS organ culture media did not alter FGF10-induced ERK activation in UGS basal epithelium but prevented FGF10-induced BrdU incorporation and blocked FGF10-induced prostatic bud formation. These results identify basal urogenital sinus epithelium cells as the key site of FGF10 action during fetal prostate development and suggest that TCDD likely acts downstream of FGFR2 and ERK to restrict UGS epithelial cell proliferation and prevent prostatic bud formation.

Key Words: **urogenital sinus; fibroblast growth factor 10; development; mouse; TCDD; prostate.**

Mouse prostate development begins *in utero* from the fetal urogenital sinus (UGS). Androgen-responsive signals from urogenital sinus mesenchyme (UGM) stimulate formation of prostate ductal progenitors, or buds, in urogenital sinus epithelium (UGE) (Cunha and Chung, 1981; Cunha and Lung, 1978). Prostatic buds are formed in three stages. The first stage is specification, and during this period, UGM signals determine the position of buds in UGE. Buds are specified in a reproducible pattern along three axes: dorsoventral, craniocaudal, and mediolateral (Lin *et al.*, 2003; Timms *et al.*, 1994). The second stage is initiation, and during this period, buds first begin to extend outward into UGM. Prostatic buds continue to extend distally into UGM during the third stage, elongation. Most prostatic buds bifurcate postnatally into branched epithelial cords, canalize, and give rise to a ductal network that is organized into separate and distinct ventral, dorsolateral, and anterior prostate lobes (Sugimura *et al.*, 1986).

Ligand-dependent activation of the aryl hydrocarbon receptor (AHR) by 2,3,7,8-tetrachlorodibenzo-*p*-dioxin (TCDD) during fetal mouse prostate development causes prostatic buds to form in an inappropriate pattern. TCDD exposure (5 μg/kg, maternal dose) on or before embryonic day (E) 15.5 completely inhibits bud formation in the ventral UGS region and causes ventral prostate agenesis (Lin *et al.*, 2003; Vezina *et al.*, 2008b). TCDD also decreases the number of buds formed in the lateral UGS region and causes buds to form inappropriately in the dorsal UGS region. The prostatic bud pattern is more severely dorsalized by TCDD when exposure occurs prior to and during bud specification (E13.5) than those occurs later in UGS development and during bud initiation (Lin *et al.*, 2003; Vezina *et al.*, 2008b). Therefore, peak UGS sensitivity to TCDD occurs before prostatic buds are formed, during bud specification. This TCDD effect is not due to androgen insufficiency in male fetuses and is not caused by direct inhibition of androgen receptor activity (Ko *et al.*, 2004b; Lin *et al.*, 2003).

The UGM is the initial site of TCDD action in the UGS. This was demonstrated by functional *Ahr* expression in UGM, and not UGE, being required for prostatic budding inhibition by TCDD (Ko *et al.*, 2004a). UGM-derived paracrine signaling molecules that stimulate bud formation, including fibroblast growth factor 10 (FGF10), are therefore likely targets of TCDD action. FGF10 is required for bud specification in multiple developing organs (Howard and Ashworth, 2006; Isaac *et al.*, 2000; Min *et al.*, 1998), including prostate. Very few prostatic buds form in *Fgf10*-null mice (Donjacour *et al.*, 2003) and in mice deficient in

one of its receptors, fibroblast growth factor receptor 2 (*Fgfr2*) (Lin *et al*., 2007). FGF10-induced activation of FGFR2 promotes phosphorylation and activation of extracellular signal–regulated kinase (ERK) 1 and ERK 2, an event required for prostatic bud formation (Kuslak and Marker, 2007).

In this report, we tested the hypothesis that TCDD disrupts FGF10-induced prostatic bud formation in male mouse UGSs. Specifically, we examined whether TCDD impairs FGF10-induced bud formation, decreases abundance of *Fgf10* or *Fgfr2*, or prevents FGF10-induced ERK activation. Our results shed light on two aspects of AHR and FGF10 signaling during mouse prostate development. First, we provide evidence that basal UGE cells are the key site of FGF10 action during prostate development in control male fetuses. Second, we demonstrate that TCDD inhibits FGF10-dependent prostatic bud formation by acting downstream of FGFR2 and ERK to disrupt basal UGE cell proliferation.

MATERIALS AND METHODS

Animals and treatments. C57BL/6J mice (Jackson Laboratory, Bar Harbor, ME) were maintained as described previously (Vezina *et al*., 2008b). All procedures were approved by the University of Wisconsin Animal Care and Use Committee and conducted in accordance with the National Institutes of Health Guide for the Care and Use of Laboratory Animals. To obtain timed-pregnant dams, female mice were paired overnight with males. The next day was considered E0.5. To obtain UGS tissues exposed *in utero* to TCDD, pregnant mice were given a single oral dose of TCDD (5 μg/kg) or vehicle (corn oil, 5 ml/kg) on E15.5. Dams were euthanized by CO_2 asphyxiation 1 day later.

UGS organ culture and bud counting. UGSs were dissected from male fetuses, placed on 0.4-μm Millicell-CM filters, and cultured as described previously (Vezina *et al*., 2008a) in media containing 5α-dihydrotestosterone (DHT; diluted from an ethanol stock solution to a final media concentration of 10nM). The following supplements were added alone or in combination to organ culture media: TCDD (Cambridge Isotopes Laboratories, Andover, MA; diluted from a dimethyl sulfoxide [DMSO] stock solution to a final media concentration of 1nM) or recombinant FGF10 protein (R&D Systems, Minneapolis, MN; diluted from a stock containing hanks balanced salt solution and bovine serum albumin [BSA] to a final media concentration of 300 ng/ml). This concentration of TCDD was shown previously to significantly decrease the number of prostatic buds formed in UGS organ culture (Allgeier *et al*., 2008) and this concentration of recombinant FGF10 protein is similar to the 200 ng/ml FGF10 concentration that was shown previously to stimulate ventral prostate development in serum-free organ culture media (Thomson and Cunha, 1999). Media for all treatment groups contained appropriate vehicle controls (final media concentration of 0.1% BSA and 0.1% DMSO), 5-bromo-2′-deoxyuridine (BrdU; diluted from an aqueous stock solution to a final media concentration of 1 μg/ml) was added to UGS organ culture media in some experiments, as indicated. Media and supplements were changed every 2 days. Some UGS tissues were harvested after 1 day for reverse transcriptase (RT)-PCR analysis and frozen in liquid nitrogen. Other UGS specimens were harvested after 3 days in culture and incubated with 1% trypsin for 90 min at 4°C. UGE was then mechanically separated from UGM and fixed in 2.5% glutaraldehyde for scanning electron microscopy. Scanning electron microscopy was performed as previously described (Lin *et al*., 2003) at the University of Wisconsin Biological and Biomaterials Preparation, Imaging, and Characterization Laboratory. Specimens were imaged from four different angles to visualize budding across the entire UGE surface. All prostatic buds were counted by the same two persons, and prostatic bud numbers were determined by averaging the total bud counts per UGS determined by these individuals.

RNA isolation and real-time RT-PCR. UGS homogenization, RNA isolation, and complementary DNA synthesis were performed as described previously (Vezina *et al*., 2008a). Real-time RT-PCR was performed as described previously (Lin *et al*., 2003) using the Roche LightCycler (Roche Applied Science, Indianapolis, IN). PCR primers were as follows: *Cyp1b1*, 5′-ACATGAGTTTCAGTTATGGCC-3′ and 5′-TTCCATTCACTGCTGAGAGC-3′; *Fgf10*, 5′-CCCTCTCCCACCCTACATTTCC-3′ and 5′-CCCACGGAGGCAGAACTCAC-3′; *Fgfr2iiib*, 5′-CAGGTAGCCCATGGTCTCAG-3′ and 5′-GGTGGTGGTCCAGTACGGTG-3′, described previously by (Nyeng *et al*., 2007); and peptidyl prolyl isomerase a (*Ppia*) 5′-TCTCTCCGTAGATGGACCTG-3′ and 5′-ATCACGGCCGATGACGAGCC-3′.

Sectional* in situ *hybridization. UGSs were fixed overnight in 4% paraformaldehyde at 4°C. UGSs were embedded in 4% SeaPlaque agarose (Biowhittaker Molecular Applications, Rockland, ME), submerged in ice-cold PBS containing 0.1% Tween 20, and sectioned (50 μm) using a vibratome fitted with a double-edged razor blade. Tissues were bleached with 6% H_2O_2 and digested with proteinase K. The probe for *Fgf10* was described previously (Bellusci *et al*., 1997) and was provided by Brigid Hogan (Duke University, Durham, NC). Antisense probes for *Fgfr2* (Miki *et al*., 1992) and *Cyp1b1* (Vezina *et al*., 2008b) were described previously. Methods for digoxigenin-11-uridine-5′-triphosphate probe labeling and immunohistochemical visualization of antisense *in situ* hybridization (ISH) probes with BM purple chromagen (Roche Applied Science) were described previously (Vezina *et al*., 2008b). The number of sections assessed for each probe is described in the "Results" section. Tissue sections were also incubated with sense ISH probes as a control measure to ensure specificity of antisense ISH probe staining patterns. Staining was not apparent in these tissue sections (results not shown).

Immunohistochemistry. Tissues were fixed in 4% paraformaldehyde, dehydrated into methanol, infiltrated with paraffin, and cut into 4-μm sections. Sections were hydrated, bleached in 10% H_2O_2, and boiled in 10mM sodium citrate, pH 6.0, for 30 min. Tissues were washed with a solution containing 25mM Tris-HCl, pH 7.5, 140mM NaCl, 2.7mM KCl, and 0.1% Tween-20. After blocking with goat sera (5%), tissues were incubated overnight at 4°C with blocking buffer containing rabbit anti-ERK (1:100; Cell Signaling Technology, Inc., Danvers, MA) or mouse anti-BrdU (1:100; Sigma-Aldrich, St Louis, MO). Tissues were washed and incubated with biotinylated goat anti-rabbit IgG (for ERK) or Alexafluor-488–conjugated goat anti-mouse IgG (for BrdU; Invitrogen, Carlsbad, CA). Signal detection for ERK was achieved by incubating tissues with streptavidin-conjugated horseradish peroxidase followed by the Vector NovaRED Peroxidase Kit as described by the manufacturer (Vector Laboratories, Burlingame, CA). Sections were counterstained with hematoxylin. The number of sections assessed for each antibody is described in the "Results" section. Tissue sections were incubated with sera from the primary antibody host animal, diluted as described for primary antibodies, as a negative control. Staining was not apparent in these tissue sections (results not shown).

Litter independence and statistical analysis. Scanning electron microscopy was conducted on UGS epithelium from three or more litters per treatment. Immunohistochemistry (IHC), ISH, and real-time RT-PCR were performed on UGSs from three to five litters per treatment. ANOVA and Student's *t*-test were conducted on untransformed data that passed Levene's test for homogeneity of variance and appeared to be normally distributed.

RESULTS

TCDD Does Not Decrease Fgf10 Messenger RNA Abundance or Alter its Distribution in the UGS of Fetal Male Mice

To test whether TCDD quantitatively decreases *Fgf10* messenger RNA (mRNA) abundance in the UGS, male fetal

mice were exposed *in utero* to vehicle or TCDD (5 μg/kg maternal oral dose on E15.5) and *Fgf10* mRNA abundance was determined in the UGS by real-time RT-PCR on E16.5 (Fig. 1A). *Cyp1b1* mRNA abundance was also examined as an index of AHR activation. Although this exposure paradigm was found previously to inhibit ventral prostatic bud formation (Vezina *et al*., 2008b), and in this study it increased *Cyp1b1* mRNA abundance (Fig. 1A), it did not significantly alter *Fgf10* abundance (Fig. 1A).

Prior to and during prostatic bud formation, *Fgf10* mRNA is expressed in two UGM domains at distal poles of the dorsoventral UGS axis (Thomson and Cunha, 1999). One of these domains is a specialized UGM tissue compartment known as the ventral mesenchymal pad, VMP (Timms *et al*., 1995). RT-PCR of whole-UGS tissue may be incapable of detecting a VMP-localized decrease in *Fgf10* abundance, even though such a decrease could impair ventral prostatic bud formation. We therefore used ISH to determine whether TCDD focally decreases *Fgf10* mRNA abundance or the size of its VMP expression domain. UGS specimens ($n = 6$ samples per exposure group, all from independent litters) were cut along the sagittal plane and sections were processed for ISH under identical conditions. *Cyp1b1* expression in vehicle-exposed UGS specimens was localized in UGM near its interface with UGE (Fig. 1B). *Cyp1b1* was not detected in the VMP of vehicle-exposed UGSs, even though *Fgf10* transcripts were abundant in this region. TCDD increased *Cyp1b1* transcript abundance in UGM and UGE and expanded *Cyp1b1* expression into the VMP where it overlapped with *Fgf10*. TCDD did not appear to decrease *Fgf10* transcript abundance or alter the *Fgf10* distribution pattern in the VMP or elsewhere in the UGS (Fig. 1B).

FGF10 Induces Prostatic Bud Formation In Vitro and TCDD Interferes with This Action

Since TCDD did not alter *Fgf10* transcript abundance in the VMP, a UGS organ culture model was used to determine if TCDD interfered with FGF10-induced bud formation. E14.5 male mouse UGSs were incubated for 3 days in organ culture medium containing the potent androgen, DHT (10nM), and either vehicle alone, recombinant FGF10 protein (300 ng/ml), TCDD (1nM), or a combination of FGF10 and TCDD. At the end of the culture period, UGE was separated from UGM and was visualized by scanning electron microscopy to reveal

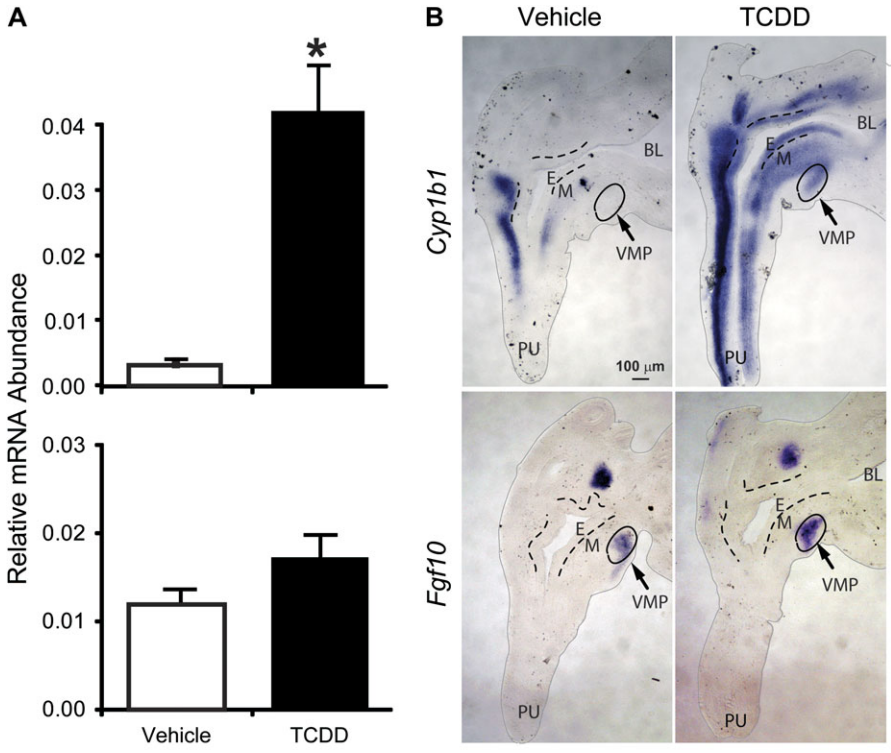

FIG. 1. *In utero* TCDD exposure increases *Cyp1b1* mRNA abundance in ventral UGM but does not alter *Fgf10* mRNA abundance or distribution in this region. Male fetal mice were exposed *in utero* to corn oil (vehicle) or TCDD (5 μg/kg maternal dose) on E15.5. (A) *Cyp1b1* and *Fgf10* mRNA abundance was determined by real-time RT-PCR on E16.5 and normalized to *Ppia* mRNA abundance. Results are mean ± SE of $n \geq 3$ independent samples per group from at least three separate litters. Significant differences between groups ($p < 0.05$) are indicated by an asterisk. (B) ISH was used to visualize the pattern of AHR-responsive *Cyp1b1* mRNA expression and *Fgf10* expression in sagittal UGS sections on E16.5. Dashed lines were added to demarcate the boundary between UGE and UGM, thin gray lines were added to show the outside edge of each UGS section, and a thin black oval indicates the approximate position of the VMP. BL. bladder; E, UGE; M, UGM; and PU, pelvic urethra.

prostatic buds protruding from the UGE (Fig. 2A). Recombinant FGF10 protein significantly increased mean prostatic bud number compared to vehicle alone, from about 27 buds to 41 buds per UGS (Fig. 2B). TCDD significantly decreased budding compared to vehicle control, from about 27 to 12 buds per UGS. When administered in combination with recombinant FGF10 protein, TCDD prevented FGF10 from inducing prostatic buds. These results suggest that AHR activation by TCDD interferes with FGF10-dependent bud induction.

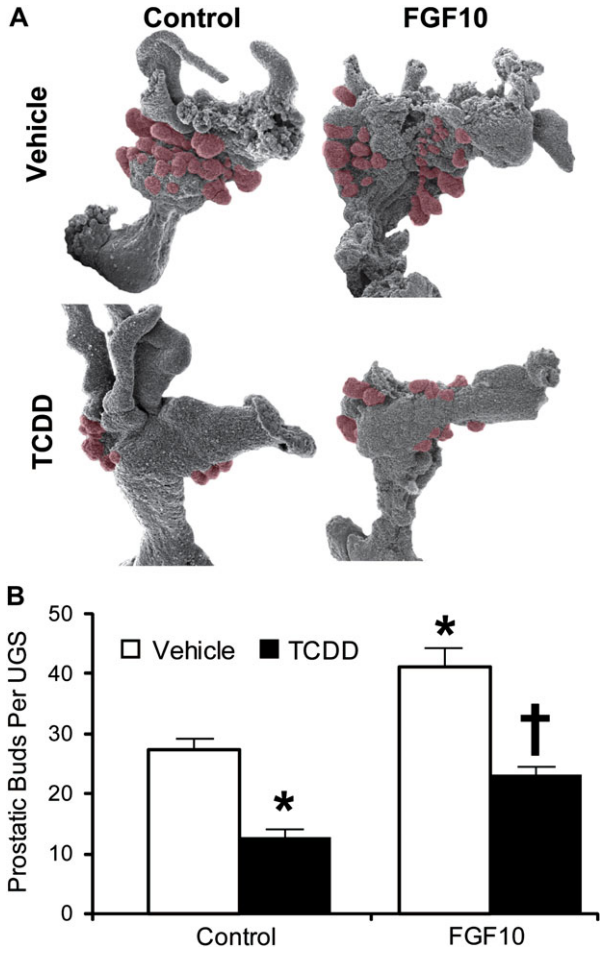

FIG. 2. Recombinant FGF10 protein significantly increases prostatic budding in UGS organ culture, and TCDD blocks this effect. UGS from E14.5 male C57BL/6J mouse fetuses were incubated for 3 days in organ culture medium containing vehicle, recombinant FGF10 protein (300 ng/ml), TCDD (1nM), or FGF10 + TCDD. Media and supplements were replenished after the second day of culture. At the end of the incubation, UGE was separated from UGM and visualized by scanning electron microscopy. (A) Micrographs of one UGE from each exposure group are shown. Prostatic buds are pseudocolored red. (B) Prostatic buds were counted using micrographs of each UGE that were taken from four separate angles in order to ensure that all prostatic buds present were counted. Results for the total number of prostatic buds per UGS are mean ± SE of $n \geq 6$ independent samples per group from at least three separate litters. The presence of an asterisk indicates a mean that is significantly different from the vehicle-treated group (control, $p < 0.05$). The presence of a dagger indicates it is significantly different from 1nM TCDD (control, $p < 0.05$).

TCDD Does Not Change Fgfr2 Transcript Abundance or Distribution and Does Not Alter FGF10-Induced ERK Activation

Since TCDD interfered with FGF10-inducible prostatic bud formation without changing *Fgf10* mRNA abundance, it was hypothesized that TCDD impaired FGF10 signaling by decreasing *Fgfr2* abundance. Male mouse fetuses were exposed *in utero* to vehicle or TCDD (5 μg/kg) on E15.5, and UGS specimens were removed 24 h later, on E16.5. *Fgfr2* mRNA abundance was assessed by RT-PCR and was unchanged by TCDD exposure (Fig. 3A), and sectional ISH revealed *Fgfr2* mRNA throughout the UGE of vehicle- and TCDD-exposed UGS specimens. TCDD did not appreciably change *Fgfr2* abundance or distribution (Fig. 3B).

It was shown previously that ligand-bound FGFR2 activates an intracellular signaling cascade involving ERK, which in turn is required for prostatic bud formation (Kuslak and Marker, 2007). We therefore looked downstream of FGFR2 to test the hypothesis that TCDD interferes with ERK activation to inhibit ventral prostatic bud formation. Male mouse fetuses were exposed *in utero* to vehicle or TCDD (5 μg/kg) on E15.5 and UGS specimens were removed 24 h later, on E16.5, embedded in paraffin and cut in the sagittal plane. ERK activation in ventral UGE was assessed by IHC with an antibody that specifically recognizes the active, phosphorylated forms of ERK 1 and 2 (Fig. 4A). The vast majority of phospho-ERK-positive cells in vehicle-exposed UGS sections were localized to UGE; very few UGM cells expressed phospho-ERK. Phospho-ERK-positive UGE cells were not evenly distributed in UGE, but instead showed a polarized distribution, with the majority of these cells clustered in the urothelial cell compartment, which is the UGE multicell layer lining the sinus space. There were substantially fewer phospho-ERK1/2-positive epithelial cells in the basal UGE cell compartment near the interface with UGM.

Very few phospho-ERK-positive UGE cells were observed following TCDD exposure on E15.5 (Fig. 4A). The mean percentage of phospho-ERK-positive UGE cells within a fixed UGS region from which ventral buds form was quantified in tissue sections from three male fetuses per treatment group. An average of 277 UGE cells per section (three sections per UGS) was examined. TCDD significantly reduced the percentage of phospho-ERK-positive epithelial cells in the ventral UGS region, from 22.6 to 4.4% (Fig. 4B). The cells with the most striking decrease in phospho-ERK expression after TCDD exposure appeared to be urothelial cells near the sinus space.

ERKs are a common intracellular target for receptor tyrosine kinases (RTKs); they are not activated exclusively by FGFR2 (McKay and Morrison, 2007). A UGS organ culture approach was used to determine if FGF10 was capable of activating ERK in urothelial cells where its activation was reduced by TCDD or if FGF10 activated ERK in a different UGE cell layer. UGS tissue specimens were removed from male fetuses at E15.5, 1

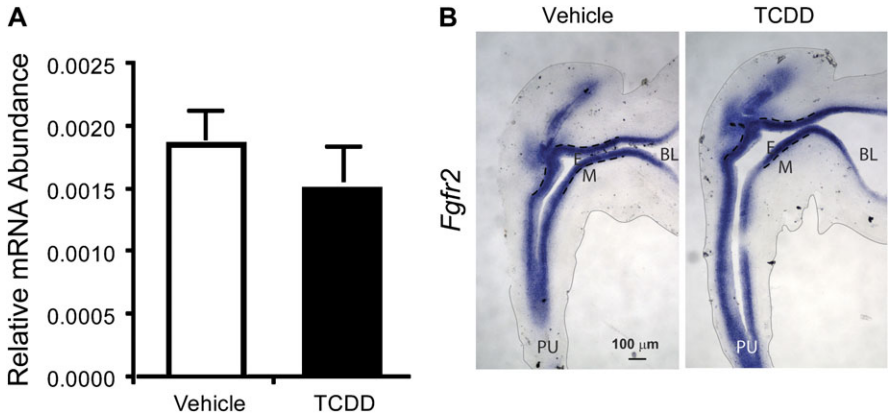

FIG. 3. *In utero* TCDD exposure does not alter *Fgfr2* mRNA abundance or distribution in UGE. Male fetal mice were exposed *in utero* to corn oil (vehicle) or TCDD (5 μg/kg maternal dose) on E15.5. (A) *Fgfr2* mRNA abundance was determined by real-time RT-PCR on E16.5 and normalized to *Ppia* mRNA abundance. Results are mean ± SE of $n \geq 3$ independent samples per group from at least three separate litters. (B) ISH was used to visualize the pattern of *Fgfr2* mRNA expression in midsagittal UGS sections on E16.5. Dashed lines were added to demarcate the boundary between UGE and UGM. Thin gray lines were added to show the outside edge of the UGS sections. BL, bladder; E, UGE; M, UGM; and PU, pelvic urethra.

day prior to the start of prostatic bud initiation, and were incubated for 3 days in organ culture medium containing 10nM DHT and vehicle alone, 1nM TCDD, 300 ng/ml recombinant FGF10 protein, or a combination of FGF10 and TCDD. Sagittal sections from cultured UGS were then examined by IHC to visualize the ERK activation pattern (Fig. 5A). There were few phospho-ERK-positive UGE cells in the vehicle control group. FGF10 increased ERK-positive cell number but only in the basal UGE cell layer. Importantly, FGF10 treatment did not appear to activate ERK in urothelial cells where it was inhibited by *in utero* TCDD exposure. TCDD by itself did not visibly alter ERK activation and did not interfere with ERK activation in basal UGE cells by FGF10. To demonstrate this quantitatively, the mean percentage of phospho-ERK-positive UGE cells within six UGE cell layers from the UGE-UGM interface was quantified in tissue sections from three UGSs per treatment (Fig. 5B). Since UGS tissues were flattened and distorted by the culture process, it was not possible to reliably determine where ventral UGS buds would form. Therefore, basal UGE cells from all prostatic budding regions were examined (an average of 260 UGE cells per section, three sections per UGS). FGF10 significantly increased the percentage of phospho-ERK-positive cells within the six basal UGE multicell layer, from 1.9 to 37.5%, and this increase was not significantly changed by TCDD (Fig. 5B). These results support the hypothesis that TCDD inhibits prostatic bud formation by impairing an FGF10-dependent end point, other than ERK activation, in basal UGE cells.

TCDD Inhibits FGF10-Induced UGE Cell Proliferation

FGF10 induces mitogenesis in other developing tissues (Bates, 2007; Nie *et al*., 2006; Sekine *et al*., 1999) and in the UGS; ERK activation is required for FGF10-induced cell proliferation (Kuslak and Marker, 2007). Since TCDD did not appear to disrupt FGF10-induced ERK activation in the UGS, it was next hypothesized that TCDD may impair FGF10-induced UGE cell proliferation to prevent prostatic buds from forming. UGS tissue specimens were removed from male fetuses at E15.5, 1 day prior to the start of prostatic bud initiation, incubated for 4 h in culture medium containing vehicle or TCDD, and then FGF10 was introduced into the culture medium and UGSs were incubated for an additional 16 h. BrdU was added to the culture medium 12 h after addition of FGF10 and remained in culture media for a total of 4 h to label cells that were in or had completed the S phase of the proliferative cycle. Sections from cultured UGSs were then examined by IHC and the mean percentage of BrdU-positive UGE cells was quantified in tissue sections from three UGSs per treatment. All UGE cells in the prostatic budding regions were examined (an average of 1588 UGE cells per section, three sections per UGS). BrdU-positive cells were observed in UGE and UGM of all treatment groups, reflecting cell proliferation in all treatments during prostatic bud formation (Fig. 6A). FGF10 significantly increased the BrdU-positive UGE cell percentage, from 1.9 to 7.3% (Fig. 6B). TCDD treatment, followed by exposure to vehicle, did not appreciably change the percentage of proliferating UGE cells when compared to UGS tissues cultured in the absence of TCDD or FGF10. However, TCDD pretreatment prevented FGF10-inducible cell proliferation (Fig. 5B). These results suggest that TCDD inhibits prostatic bud formation by interfering with FGF10-inducible basal UGE cell proliferation.

DISCUSSION

We previously showed that fetal and neonatal TCDD exposure inhibited mouse prostatic budding and permanently reduced prostate size and duct number (Ko *et al*., 2002; Lin *et al*., 2003). We demonstrated that prostatic buds are most

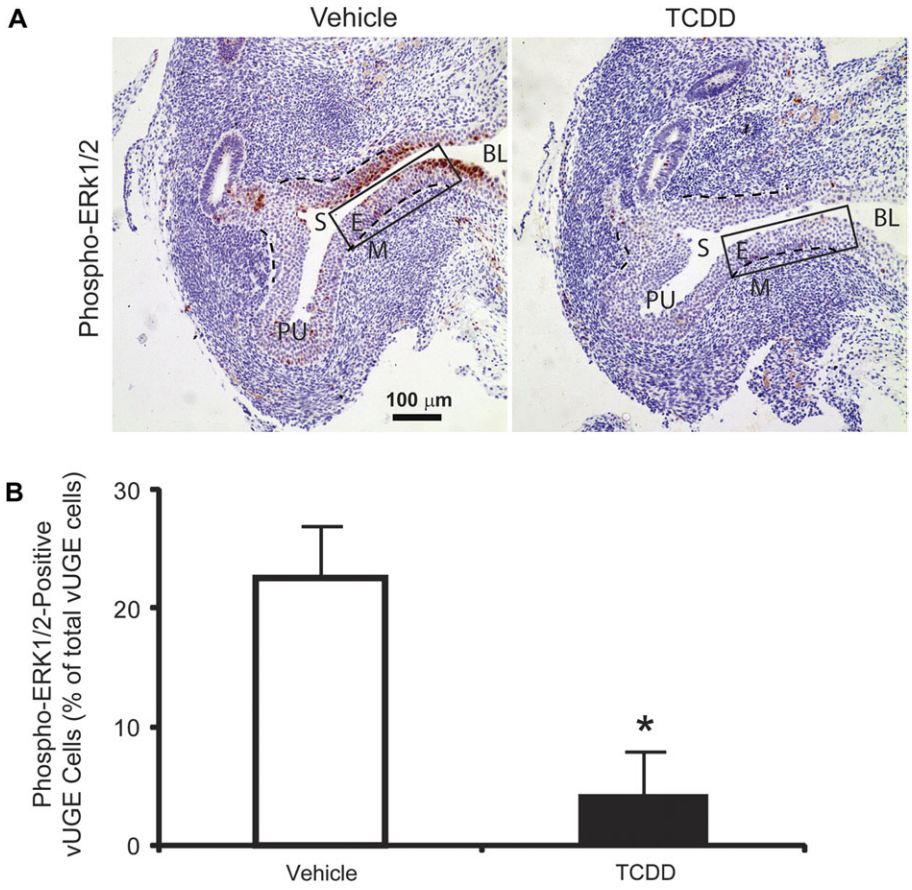

FIG. 4. *In utero* TCDD exposure significantly decreases ERK activation in UGE cells. Male fetal mice were exposed *in utero* to corn oil (vehicle) or TCDD (5 μg/kg maternal dose) on E15.5. (A) IHC was used to visualize the pattern of activated phosphorylated ERK protein expression (red) in sagittal UGS sections on E16.5. Results are representative of at least three UGSs per group. Dashed lines were added to demarcate the boundary between UGE and UGM. BL, bladder; E, UGE; M, UGM; and PU, pelvic urethra; S, sinus space. (B) The percentage of ventral UGE (vUGE) cells expressing active phosphorylated ERK (red) was determined in the ventral prostatic budding region (inside black rectangle) by counting separately all the vUGE cells and all the red-stained vUGE cells on three sections per UGS. Results are mean ± SE of $n \geq 3$ UGSs per group, each from a different litter. Significant differences among groups ($p < 0.05$) are indicated by an asterisk.

vulnerable to inhibition by TCDD during their specification and prior to prostatic bud initiation (Vezina *et al*., 2008b). This led us to hypothesize that TCDD impairs prostatic budding by disrupting developmental patterning signals during prostatic bud specification. Organogenesis is generally regulated by morphogenetic signals distributed in specific patterns about craniocaudal, dorsoventral, and mediolateral axes (Meinhardt, 2008). TCDD appears to interfere with signals along the dorsoventral axis, yielding a dorsalized prostatic UGS where buds are inappropriately clustered on the dorsal surface, reduced in number on the lateral surface, and absent from the ventral surface (Lin *et al*., 2003; Vezina *et al*., 2008b).

In the present study, we provide evidence that TCDD prevents FGF10-induced prostatic bud formation and cell proliferation. FGF10 signaling has been implicated in the fetal basis of adult prostate disease (Huang *et al*., 2005) and is active in prostate cancer (Memarzadeh *et al*., 2007). TCDD inhibited FGF10-induced UGE cell proliferation and prostatic bud formation without altering UGS abundance or regional distribution of *Fgf10*-, *Fgfr2*-, or FGF10-induced ERK activation. It therefore appears that TCDD acts downstream of *Fgfr2*, and likely also downstream of ERK, to impair prostatic budding. A region-specific inhibition of *Fgf10*-induced budding by TCDD may in part be responsible for dorsalizing the prostatic bud pattern in fetal male mice.

AHR activation by TCDD during fetal mouse development appears to cause latent adverse affects on prostate biology that permanently reprogram the prostate and increase disease susceptibly in adulthood. *In utero* and lactational TCDD exposure caused male mice to inappropriately retain a high degree of prostate androgen dependence and increased the frequency of hyperplastic prostate growth lesions when these animals reached senescence (Fritz *et al*., 2005). *In utero* and lactational TCDD exposure also increases neuroendocrine prostate tumor incidence in 140-day-old TRAMP mice (Lin *et al*., 2009). It is imperative to understand mechanisms of

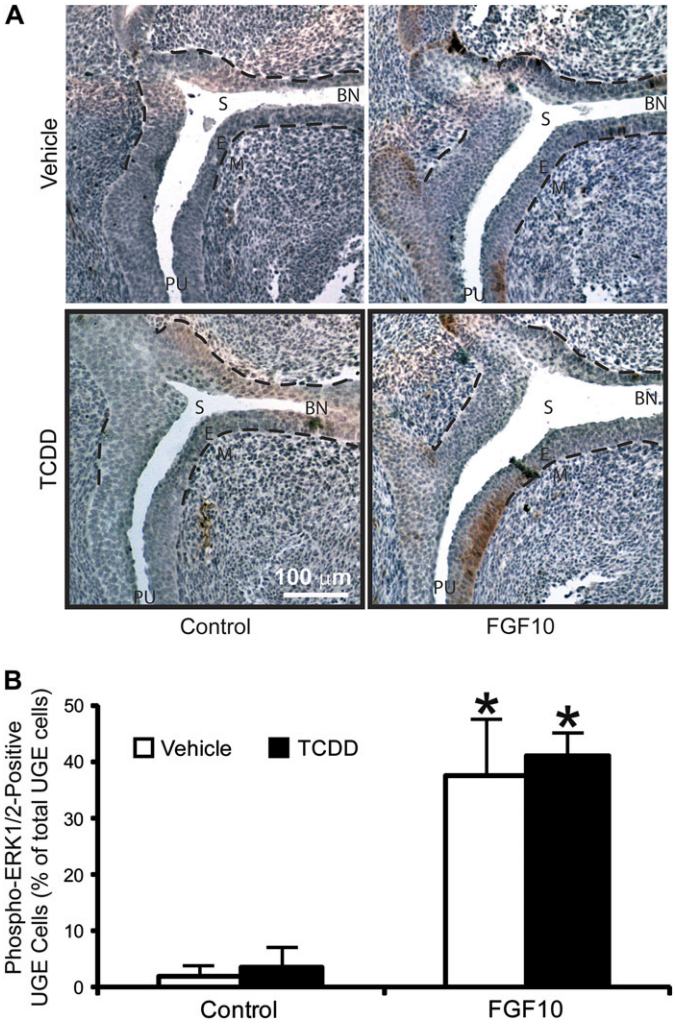

FIG. 5. TCDD does not prevent ERK activation by recombinant FGF10 protein in the prostatic budding region of cultured UGS. UGS from E14.5 male C57BL/6J mouse fetuses were incubated for 3 days in organ culture medium containing vehicle, recombinant FGF10 protein (300 ng/ml), TCDD (1nM), or FGF10 + TCDD. (A) IHC was then used to visualize the pattern of activated phosphorylated ERK protein expression (red) in the prostatic budding region of sagittal UGS sections. Dashed lines demarcate the boundary between UGE and UGM in the prostatic budding region. E, UGE; M, UGM; PU, pelvic urethra; BL, bladder; and S, sinus space. (B) The percentage of UGE cells expressing active phosphorylated ERK (red) was determined in the prostatic budding region by counting all the UGE cells and all the red-stained UGE cells in a six-cell-thick layer of UGE cells adjacent to the UGE-UGM interface (dashed line). Three sections per UGS were analyzed. Results are mean ± SE of $n \geq 3$ UGSs per group, each from a different litter. Significant differences among groups ($p < 0.05$) are indicated by an asterisk.

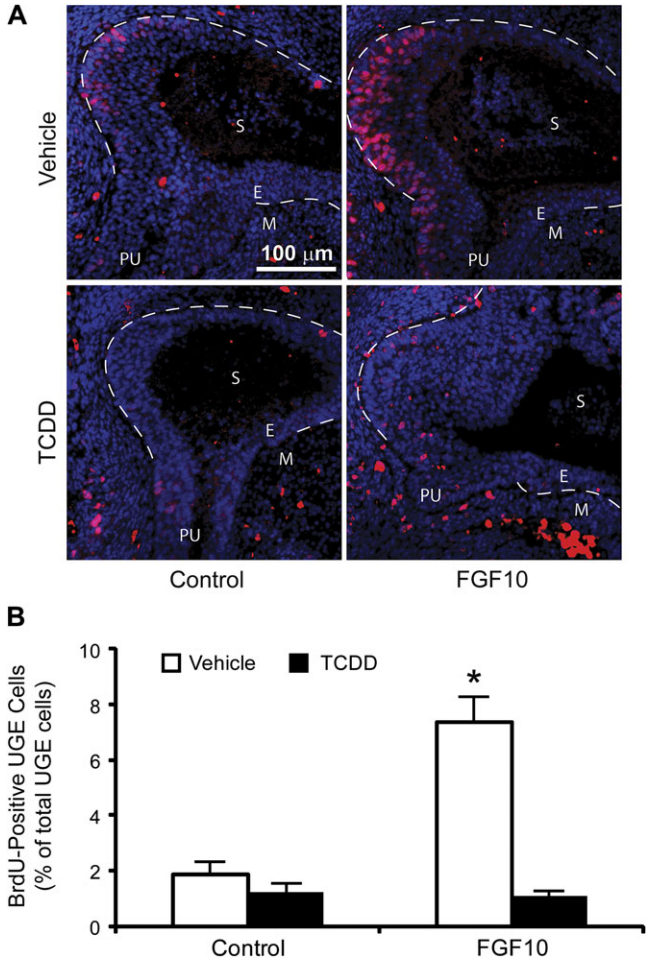

FIG. 6. TCDD inhibits FGF10-dependent cell proliferation in UGS organ culture. UGS from E15.5 male C57BL/6J mouse fetuses were incubated for 4 h in organ culture medium containing vehicle or 1nM TCDD. Vehicle or 300 ng/ml recombinant FGF10 protein was then added to organ culture medium, and tissues were cultured for an additional 16 h. BrdU was added to the culture medium after 12 h. (A) Sections from cultured UGSs were then examined by IHC and (B) BrdU-positive UGE cells (red) were quantified as a percentage of the total number of prostatic UGE cells (nuclei are blue) in tissue sections from three UGSs per treatment group. Three sections per UGS were examined. Dashed lines were added to demarcate the boundary between UGE and UGM in the UGS proper. The percentage of BrdU-positive UGE cells was determined in the UGE region circumscribed by these dashed lines. E, UGE; M, UGM; PU, pelvic urethra; and S, sinus space. Results are mean ± SE of $n \geq 3$ UGSs per group, each from a different litter. Significant differences among groups ($p < 0.05$) are indicated by an asterisk.

TCDD action in the fetal UGS because of this growth period's relevance to prostate health.

To understand how TCDD inhibits FGF10-induced prostatic budding, it is necessary to understand how budding is induced by FGF10. However, there is little evidence for how this occurs. In postnatal rat prostate, FGF10 activates *sonic hedgehog* and *homeobox b13* transcription to regulate ductal branching morphogenesis (Pu *et al.*, 2007) but it is unclear whether FGF10 serves the same function during prenatal prostatic bud formation. To further understand the mechanism by which FGF10 signaling is reduced by TCDD during prostatic budding, the FGF10 signaling pathway must be resolved in greater detail, specifically the downstream events leading to FGF10-dependent UGE cell proliferation must be identified. Kuslak and Marker (2007) reported that FGF10 activates ERK in mouse UGS and that this event is required for FGF10-induced cell proliferation. Our results build upon this

observation by revealing that ERK is induced selectively by FGF10 in basal UGE cells, which is also where FGF10 most strongly induced cell proliferation in UGS organ culture. With this new knowledge of basal UGE cells being a target of FGF10 signaling, it will now be possible to elucidate, in future studies, downstream signals mediated by FGF10 in this UGE multicell layer. There are already some candidate factors that may be mediating FGF10 signaling targets in these cells. The ERK activation pattern by FGF10 in UGE cells is similar to that described previously for other proteins required for prostate development, including SOX9 (Thomsen *et al*., 2008), FOXA2 (Mirosevich *et al*., 2005), and transformation-related protein 63 (Cook *et al*., 2007). SOX9, which is required for the normal FGFR2 expression pattern in UGS (Thomsen *et al*., 2008), appears to be upstream of FGF10 signaling but the relationships between FGFR2, P63, and FOXA2 remain unknown.

An unexpected finding in this study was that TCDD inhibited ERK activation in urothelial cells, which do not appear to be highly FGF10 responsive at the gestational age that our study was conducted. TCDD was reported previously to induce AHR-responsive *Cyp1a1* mRNA expression in urothelial cells (Vezina *et al*., 2008b), and although this cell population does not play a known role in prostatic bud formation, it is a direct target for TCDD action. Intracellular signals from multiple RTKs converge on the map kinase signaling pathway to elicit intracellular responses (McKay and Morrison, 2007). TCDD may inhibit one of these receptor-mediated signals, thereby decreasing ERK activation in urothelial cells. Epidermal growth factor and transforming growth factor (TGF) α are expressed in fetal male rat UGS (Saito and Mizuno, 1995), both activate ERK in prostate (Hagan *et al*., 2004; Putz *et al*., 1999), and both appear to regulate prostatic bud formation in the mouse (Abbott *et al*., 2003). Additional RTKs or their ligands have been identified in fetal male UGS, including TGFβ (Timme *et al*., 1994), colony-stimulating factor receptor (Paine-Saunders *et al*., 2002), and keratinocyte growth factor (Gao *et al*., 2005), but the activation pattern of these RTKs is unknown. Future studies will determine if these factors activate ERK in developing urothelial cells and investigate whether TCDD-induced ERK inhibition in urothelial cells influences their ability to differentiate.

FUNDING

National Institutes of Health (R37 ES01332 and P50 DK065303 to R.E.P., F32 ES014284 and K01 DK083425 to C.M.V., F31 HD049323 to S.H.A.).

ACKNOWLEDGMENTS

We thank Dr Ralph Albrecht for assistance with scanning electron microscopic imaging.

REFERENCES

Abbott, B. D., Lin, T. M., Rasmussen, N. T., Albrecht, R. M., Schmid, J. E., and Peterson, R. E. (2003). Lack of expression of EGF and TGF-alpha in the fetal mouse alters formation of prostatic epithelial buds and influences the response to TCDD. *Toxicol. Sci.* **76,** 427–436.

Allgeier, S. H., Lin, T. M., Vezina, C. M., Moore, R. W., Fritz, W. A., Chiu, S. Y., Zhang, C., and Peterson, R. E. (2008). WNT5A selectively inhibits mouse ventral prostate development. *Dev. Biol.* **324,** 10–17.

Bates, C. M. (2007). Role of fibroblast growth factor receptor signaling in kidney development. *Pediatr. Nephrol.* **22,** 343–349.

Bellusci, S., Grindley, J., Emoto, H., Itoh, N., and Hogan, B. L. (1997). Fibroblast growth factor 10 (FGF10) and branching morphogenesis in the embryonic mouse lung. *Development* **124,** 4867–4878.

Cook, C., Vezina, C. M., Allgeier, S. H., Shaw, A., Yu, M., Peterson, R. E., and Bushman, W. (2007). Noggin is required for normal lobe patterning and ductal budding in the mouse prostate. *Dev. Biol.* **312,** 217–230.

Cunha, G. R., and Chung, L. W. (1981). Stromal-epithelial interactions–I. Induction of prostatic phenotype in urothelium of testicular feminized (Tfm/y) mice. *J. Steroid Biochem.* **14,** 1317–1324.

Cunha, G. R., and Lung, B. (1978). The possible influence of temporal factors in androgenic responsiveness of urogenital tissue recombinants from wild-type and androgen-insensitive (*Tfm*) mice. *J. Exp. Zool.* **205,** 181–193.

Donjacour, A. A., Thomson, A. A., and Cunha, G. R. (2003). FGF-10 plays an essential role in the growth of the fetal prostate. *Dev. Biol.* **261,** 39–54.

Fritz, W. A., Lin, T. M., Moore, R. W., Cooke, P. S., and Peterson, R. E. (2005). In utero and lactational 2,3,7,8-tetrachlorodibenzo-p-dioxin exposure: effects on the prostate and its response to castration in senescent C57BL/6J mice. *Toxicol. Sci.* **86,** 387–395.

Gao, N., Ishii, K., Mirosevich, J., Kuwajima, S., Oppenheimer, S. R., Roberts, R. L., Jiang, M., Yu, X., Shappell, S. B., Caprioli, R. M., *et al.* (2005). Forkhead box A1 regulates prostate ductal morphogenesis and promotes epithelial cell maturation. *Development* **132,** 3431–3443.

Hagan, M., Yacoub, A., and Dent, P. (2004). Ionizing radiation causes a dose-dependent release of transforming growth factor alpha in vitro from irradiated xenografts and during palliative treatment of hormone-refractory prostate carcinoma. *Clin. Cancer Res.* **10,** 5724–5731.

Howard, B., and Ashworth, A. (2006). Signalling pathways implicated in early mammary gland morphogenesis and breast cancer. *PLoS Genet.* **2,** e112.

Huang, L., Pu, Y., Alam, S., Birch, L., and Prins, G. S. (2005). The role of Fgf10 signaling in branching morphogenesis and gene expression of the rat prostate gland: lobe-specific suppression by neonatal estrogens. *Dev. Biol.* **278,** 396–414.

Isaac, A., Cohn, M. J., Ashby, P., Ataliotis, P., Spicer, D. B., Cooke, J., and Tickle, C. (2000). FGF and genes encoding transcription factors in early limb specification. *Mech. Dev.* **93,** 41–48.

Ko, K., Moore, R. W., and Peterson, R. E. (2004a). Aryl hydrocarbon receptors in urogenital sinus mesenchyme mediate the inhibition of prostatic epithelial bud formation by 2,3,7,8-tetrachlorodibenzo-p-dioxin. *Toxicol. Appl. Pharmacol.* **196,** 149–155.

Ko, K., Theobald, H. M., Moore, R. W., and Peterson, R. E. (2004b). Evidence that inhibited prostatic epithelial bud formation in 2,3,7,8-tetrachlorodibenzo-p-dioxin-exposed C57BL/6J fetal mice is not due to interruption of androgen signaling in the urogenital sinus. *Toxicol. Sci.* **79,** 360–369.

Ko, K., Theobald, H. M., and Peterson, R. E. (2002). In utero and lactational exposure to 2,3,7,8-tetrachlorodibenzo-p-dioxin in the C57BL/6J mouse prostate: lobe-specific effects on branching morphogenesis. *Toxicol. Sci.* **70,** 227–237.

Kuslak, S. L., and Marker, P. C. (2007). Fibroblast growth factor receptor signaling through MEK-ERK is required for prostate bud induction. *Differentiation* **75,** 638–651.

Lin, T.-M., Fritz, W. A., Safe, S., and Peterson, R. E. (2009). TCDD and the selective aryl hydrocarbon receptor (AhR) modulators indole-3-carbinol

(I3C) and 3,3′-diindolylmethane (DIM) regulate prostate tumorigenesis in TRAMP mice. *Toxicol. Sci.* **108,** 626.

Lin, T. M., Rasmussen, N. T., Moore, R. W., Albrecht, R. M., and Peterson, R. E. (2003). Region-specific inhibition of prostatic epithelial bud formation in the urogenital sinus of C57BL/6 mice exposed *in utero* to 2,3,7,8-tetrachlorodibenzo-*p*-dioxin. *Toxicol. Sci.* **76,** 171–181.

Lin, Y., Liu, G., Zhang, Y., Hu, Y. P., Yu, K., Lin, C., McKeehan, K., Xuan, J. W., Ornitz, D. M., Shen, M. M., *et al.* (2007). Fibroblast growth factor receptor 2 tyrosine kinase is required for prostatic morphogenesis and the acquisition of strict androgen dependency for adult tissue homeostasis. *Development* **134,** 723–734.

McKay, M. M., and Morrison, D. K. (2007). Integrating signals from RTKs to ERK/MAPK. *Oncogene* **26,** 3113–3121.

Meinhardt, H. (2008). Models of biological pattern formation: from elementary steps to the organization of embryonic axes. *Curr. Top. Dev. Biol.* **81,** 1–63.

Memarzadeh, S., Xin, L., Mulholland, D. J., Mansukhani, A., Wu, H., Teitell, M. A., and Witte, O. N. (2007). Enhanced paracrine FGF10 expression promotes formation of multifocal prostate adenocarcinoma and an increase in epithelial androgen receptor. *Cancer Cell* **12,** 572–585.

Miki, T., Bottaro, D. P., Fleming, T. P., Smith, C. L., Burgess, W. H., Chan, A. M., and Aaronson, S. A. (1992). Determination of ligand-binding specificity by alternative splicing: two distinct growth factor receptors encoded by a single gene. *Proc. Natl. Acad. Sci. U.S.A.* **89,** 246–250.

Min, H., Danilenko, D. M., Scully, S. A., Bolon, B., Ring, B. D., Tarpley, J. E., DeRose, M., and Simonet, W. S. (1998). Fgf-10 is required for both limb and lung development and exhibits striking functional similarity to Drosophila branchless. *Genes Dev.* **12,** 3156–3161.

Mirosevich, J., Gao, N., and Matusik, R. J. (2005). Expression of *Foxa* transcription factors in the developing and adult murine prostate. *Prostate* **62,** 339–352.

Nie, X., Luukko, K., and Kettunen, P. (2006). FGF signalling in craniofacial development and developmental disorders. *Oral Dis.* **12,** 102–111.

Nyeng, P., Norgaard, G. A., Kobberup, S., and Jensen, J. (2007). FGF10 signaling controls stomach morphogenesis. *Dev. Biol.* **303,** 295–310.

Paine-Saunders, S., Viviano, B. L., Economides, A. N., and Saunders, S. (2002). Heparan sulfate proteoglycans retain Noggin at the cell surface: a potential mechanism for shaping bone morphogenetic protein gradients. *J. Biol. Chem.* **277,** 2089–2096.

Pu, Y., Huang, L., Birch, L., and Prins, G. S. (2007). Androgen regulation of prostate morphoregulatory gene expression: Fgf10-dependent and -independent pathways. *Endocrinology* **148,** 1697–1706.

Putz, T., Culig, Z., Eder, I. E., Nessler-Menardi, C., Bartsch, G., Grunicke, H., Uberall, F., and Klocker, H. (1999). Epidermal growth factor (EGF) receptor blockade inhibits the action of EGF, insulin-like growth factor I, and a protein kinase A activator on the mitogen-activated protein kinase pathway in prostate cancer cell lines. *Cancer Res.* **59,** 227–233.

Saito, M., and Mizuno, T. (1995). Le facteur de croissance de l'epiderme (EGF) peut induire des bourgeons prostatiques en l'absence d'androgenes. [Epidermal growth factor (EGF) can induce prostatic buds in the absence of androgens]. *C.R. Seances Soc. Biol. Fil.* **189,** 637–641.

Sekine, K., Ohuchi, H., Fujiwara, M., Yamasaki, M., Yoshizawa, T., Sato, T., Yagishita, N., Matsui, D., Koga, Y., Itoh, N., *et al.* (1999). Fgf10 is essential for limb and lung formation. *Nat. Genet.* **21,** 138–141.

Sugimura, Y., Cunha, G. R., and Donjacour, A. A. (1986). Morphogenesis of ductal networks in the mouse prostate. *Biol. Reprod.* **34,** 961–971.

Thomsen, M. K., Butler, C. M., Shen, M. M., and Swain, A. (2008). Sox9 is required for prostate development. *Dev. Biol.* **316,** 302–311.

Thomson, A. A., and Cunha, G. R. (1999). Prostatic growth and development are regulated by FGF10. *Development* **126,** 3693–3701.

Timme, T. L., Truong, L. D., Merz, V. W., Krebs, T., Kadmon, D., Flanders, K. C., Park, S. H., and Thompson, T. C. (1994). Mesenchymal-epithelial interactions and transforming growth factor-beta expression during mouse prostate morphogenesis. *Endocrinology* **134,** 1039–1045.

Timms, B. G., Lee, C. W., Aumuller, G., and Seitz, J. (1995). Instructive induction of prostate growth and differentiation by a defined urogenital sinus mesenchyme. *Microsc. Res. Tech.* **30,** 319–332.

Timms, B. G., Mohs, T. J., and Didio, L. J. (1994). Ductal budding and branching patterns in the developing prostate. *J. Urol.* **151,** 1427–1432.

Vezina, C. M., Allgeier, S. H., Fritz, W. A., Moore, R. W., Strerath, M., Bushman, W., and Peterson, R. E. (2008a). Retinoic acid induces prostatic bud formation. *Dev. Dyn.* **237,** 1321–1333.

Vezina, C. M., Allgeier, S. H., Moore, R. W., Lin, T. M., Bemis, J. C., Hardin, H. A., Gasiewicz, T. A., and Peterson, R. E. (2008b). Dioxin causes ventral prostate agenesis by disrupting dorsoventral patterning in developing mouse prostate. *Toxicol. Sci.* **106,** 488–496.